A probabilistic particle replacement model to simulate bulk material degradation during conveying processes using DEM

Michael Denzel
Research Assistant
University of Leoben
Chair of Mining Engineering and Mineral Economis

Michael Prenner
Senior Scientis
University of Leoben
Chair of Mining Engineering and Mineral Economis

Nikolaus A. Sifferlinger
Professor
University of Leoben
Chair of Mining Engineering and Mineral Economis

Due to mechanical stress during transport and storage, bulk material partly degrades and fines are produced. This can be problematic in various applications and is often responsible for high costs, energy consumption and emissions. In this work a model for the discrete element method is presented to simulate particle breakage during conveying processes. The breakage model is based on the particle replacement method. In contrast to other particle replacement models, mass and volume remain constant. The model has been verified and validated by a trial of shatter tests with blast furnace sinter. High mass flows and further breakage of fragments for processes with several damaging events, as found in industrial applications, can also be simulated. An application of this model is presented, where two different transfer chutes are compared with regard to material degradation. Simulation and test results are consistent.

Keywords: *particle breakage, discrete element method, voronoi tessellation, transfer chute, fines, blast furnace sinter*

1. INTRODUCTION

Due to mechanical stress during transport and storage, bulk material partly degrades and fines are produced [1–6]. This can be problematic in various applications and is often responsible for high costs, energy consumption and emissions [7]. Especially at transfer points the bulk material has a high energy content and kinetic energy is transferred into material degradation and equipment wear [8, 9]. Undesired particle breakage may also occur during processing, at conventional screens for example. In coal mining, for example, material degradation is also avoided due to the risk of dust explosions and air pollution.

Material degradation is particularly critical during transport and storage processes of blast furnace sinter. Small-grained input materials are agglomerated in the sinter process. During transport and storage the sinter passes through various conveyors, transfer chutes, coolers, sieves and bunkers, where it degrades partly. To ensure a sufficient gas flow in the blast furnace a minimum grain size is required. Before the sinter is charged into the blast furnace, fines are screened out and returned to the sinter plant again. These so-called return fines are 6% of the total sinter mass flow in EU-average [10]. Thus a reduction of return fines during transport and storage would lead to massive savings in costs and CO_2-emissions due to the highly energy consuming sinter process [7]. A study on the generation of return fines during transportation was made in [11].

The following work was conducted within the project MinSiDeg (Minimisation of Sinter Degradation) in coorperation with industrial partners. The here described breakage model for DEM (Discrete Element Method) is applied on blast furnace sinter, but is generally applicable for breakable bulk material. The model was presented for the first time in [12]. Simulating particle breakage allows to analyze and optimize existing conveying and storage equipment with regard to bulk material degradation and supports the development of innovative particle preserving concepts.

2. ANALYSIS OF BREAKAGE BEHAVIOUR

In order to analyse the breakage behaviour of the bulk material, single-particle tests are conducted with an especially developed test rig, described in 2.1. The development process and a detailed description of the test rig is provided in [13].

In total 3500 tests with blast furnace sinter of different particle sizes from 10 to 50mm and from different manufacturers were conducted. For breakage simulations, the particle size distribution (PSD) after the damaging event is relevant and is described in 2.2. Additionally, this test method allows to determine the following properties in dependence of mass-specific energy input to characterize breakage behaviour, which are described in detail in [13]: breakage probability as suggested in [14], breakage characteristics with the well-established t_n-modeling concept [15–17] based on [18–20], absolute and relative fines generation, variations in fines generation. Furthermore, a general size-independent return fines production curve could be constructed in [13].

Correspondence to: Michael Denzel, Research Assistant
Chair of Mining Engineering and Mineral Economics, University of Leoben
Franz-Josef-Straße 18, 8700 Leoben, Austria
E-mail: michael.denzel@unileoben.ac.at
DOI: https://doi.org/10.34901/mul.pub.2023.02

2.1. Test method

One of the main causes for material degradation during transport are impacts against a chute or another particle. Thus, accelerating the particle itself and shooting it against a target was considered closer to reality than a drop-weight, pendulum hammer test [21, 22] or a pressure bar [23]. A drop-weight test would be simple and is an established test method to characterize comminution behaviour [15, 24–31], but energy input by two contacting surfaces could result in different fragmentation behavior. A rapid method for impact testing is a rotary impact tester [18, 32–34], but is relatively expensive and less suitable for detailed single-particle test evaluation. Single-particle test methods are evaluated in [35].

For a detailed determination of breakage behavior, single particle tests are necessary and a wide range of energies should be covered. Furthermore, the particles must be accelerated carefully to avoid breakage during acceleration. The major challenge in single-particle testing of various bulk materials is that due to eventual heterogeneity and varying particle shapes, a reliable statement about breakage behavior can only be achieved by high sample numbers [29]. This requires a high grade of automation, but undefined shape and eventual fragility of particles complicate handling. Consequently, a highly-automated single-particle impact tester with separation, weighing system, two different acceleration concepts for low and high energy testing with integrated automated fragment analysis was developed, seen in Figure 1. [13]

Core element of this test rig is an especially developed air cannon, which accelerates the particles against a target, similar to devices in [36–39]. In contrast to these devices, the here developed air cannon propels the particles in a sabot to ensure high reproducibility and fine adjustment of impact speeds with varying particle shapes.

Figure 1. Automated single-particle impact tester

In Figure 2 a flow diagram and an overview of the test rig is presented. A bulk sample is placed into the vibratory bowl feeder, where the particles are separated along a spiral. As a particle drops out and is detected by a light gate, the feeder is switched off and the particle slides along guide plates onto the padded weighing station. After weighing, the particle is carefully pushed by a pneumatic cylinder and slides into the air cannon. To ensure correct placement in the cannon, the particle is guided by a moveable system of guide plates, which is coupled to the movement of the pneumatic cylinder [40]. The loading closure of the cannon is also moved pneumatically. Meanwhile the air tank has been filled with the desired pressure. As the shooting valve opens, the sabot in the cannon is accelerated and the particle is fired against a target in a housing, which is a 20mm thick steel plate in this case. To allow investigations regarding equipment materials, the interacting target is easily replaceable. These can be wear or damping investigations, for example. The particle speed is measured by two Arduino-based self-built light gates directly after the muzzle and in front of the steel plate. With this air cannon particles up to 50mm can be accelerated to 4-26m/s, which is equivalent to 8-338J/kg. After collision the fragments are led via several padded slides into the vibrating sorter, where the received particles are carefully sorted by size. Under the vibrating sorter collecting boxes on weigh cells are placed for each fraction. All weigh cells are zero balanced before a new shot is fired. The weights of each fraction after breakage (m_1 to m_7 for particle size fractions <6.3, 6.3-10, 10-16, 16-25, 25-40, 40-50 and >50mm), the initial particle mass (m_0) and the measured velocity is then saved to a CSV-file on an SD-card. Consequently, particle size distribution, fines production and other breakage properties can be determined as functions of impact energy and initial particle mass. After the data has been saved, the bowl feeder starts again and the process begins anew. The whole process takes approximately one minute. [13]

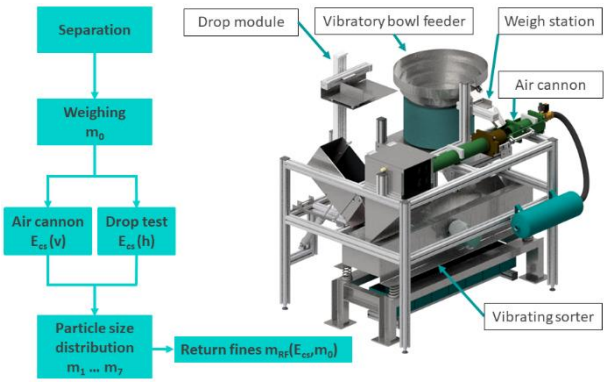

Figure 2. Concept of the automated single-particle impact tester

For tests involving particles >50mm, an additional drop module is implemented. Here the particles are placed manually on the drop module. The height of the drop module is adjusted by a spindle drive and a weighing platform is integrated. The drop height is 300-900mm, which is equivalent to 2.9-8.8J/kg. After weighing the particle is carefully pushed and falls into a box with a replaceable target at the bottom, in this case a 20mm steel plate. While the box is tilted, the front

side of the box opens with a couple mechanism and the fragments slide into the padded receiving section of the vibrating sorter. From here onwards, the automated fragment analysis is the same procedure as for high energy tests by air cannon. [13]

2.2. Results

For DEM breakage simulations the fragment size distribution in dependence after the damaging event is relevant. In Figure 3 the fragment size distribution of blast furnace sinter particles of 25-40mm initial size is exemplary depicted in dependence of the mass specific impact energy. First model verifications and validations were performed with this material. Hereby, 180 particles were tested on 6 different specific energy levels. Each data point represents the average fragment size distribution of 30 valid tests. For more homogeneous materials than blast furnace sinter, less tests would be sufficient. In this case the mass fraction of the initial particle size reduces exponentially and mass fractions of small particle sizes and fines increase almost linearly with specific impact energy. Further results and findings regarding breakage behaviour of blast furnace sinter are provided in [13, 41, 42].

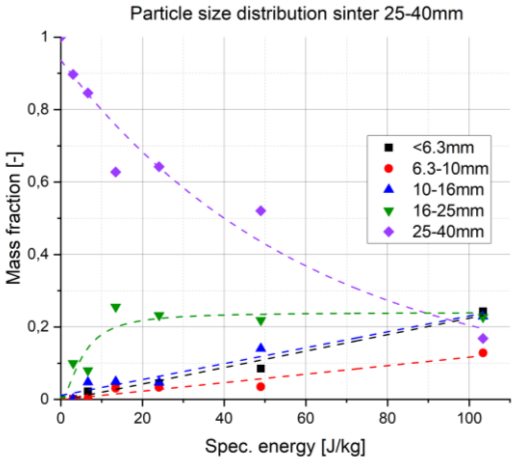

Figure 3. Fragment size distribution of blast furnace sinter particles of 25-40mm initial size in dependence of the mass specific impact energy

3. SIMULATION MODEL

Several analytical models are provided to describe bulk material degradation, especially steelmaking materials [43, 44] including fines production [22]. Also various computer simulations including continuum damage mechanics were carried out to simulate individual particle breakage [45–47]. A model for pellet degradation by impact, including repeated impacts, is described in [38]. However, to simulate bulk material behaviour, DEM is well established. Thus, to simulate bulk material degradation of high mass flows with high accuracy using DEM, a novel particle breakage model was developed, which is based on a probabilistic particle replacement method combined with voronoi tessellation.

3.1. The particle replacement method

The particle replacement method, originally proposed by Cleary [48], was successfully used to describe particle breakage under confined conditions [49–51], in geotechnical applications [52, 53] and in comminution equipment including different types of crushers [54–56]. Hereby, the particles are replaced by several smaller particles at a damaging event. This has the advantage that fragment size distributions can be defined, which leads to high accuracy and no additional calibration is needed like for other breakage models. For the bonded particle model [30, 57], for example, bond calibration requires great effort. The disadvantage of the particle replacement model is, however, the volume loss when a large sphere is replaced by several smaller spheres. To ensure mass constancy, the fragment density was adjusted in [58], which is negligible in mills and crushers, but less suitable for conveying processes with high mass flows because flow behaviour and loads on conveying equipment would be distorted. In [59] volume constancy is ensured by overlapping the following smaller spheres and defining damping factors for the following time steps to avoid explosions. Thus, the fragments slowly drift apart, which could lead to "swelling effects" in the bulk sample and could be disadvantageous for simulating conveying processes.

3.2. A probabilistic particle replacement model with voronoi tesselation

Depending on the stress, initial particles are probabilistically replaced by different following particles, similar to [59]. In contrast to [59] and other particle replacement models, the initial particle is replaced by different breakage patterns instead of several smaller spheres. The different breakage patterns have the same mass and volume as the initial particle, which ensures mass and volume constancy. The breakage patterns are pre-defined and are exact copies of the initial particle, but are tessellated with the voronoi algorithm [60–62], see Figure 4. In this case initial particles are of spherical shape, but can be any convex mesh shape. The voronoi algortihm is an efficient way to tessellate areas or volumes. For voronoi tessellation randomly distributed points (seeds) are generated. Then the area or volume is divided in the middle of two neighbouring seeds. Thus, the average fragment size depends on the number of seeds. Those fragments are sharp-edged convex mesh particles and of random shape. This requires more computing power and in some cases smaller simulation time steps than with spheres, but ensures mass and volume constancy.

In Figure 4 the here described example of blast furnace sinter of 40mm initial particle size is depicted. 4 different breakage patterns were defined for the different resulting fragment sizes (25mm, 16mm, 10mm, 6mm). To reduce computing power, fines are represented larger and summarised as 6mm-fragments.

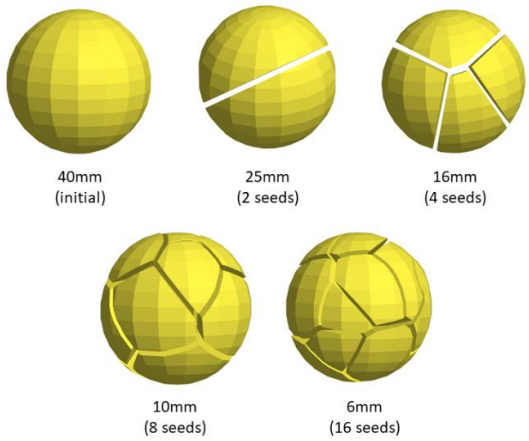

Figure 4. Voronoi-tesselated convex mesh particle of spherical shape (exploded view for better visualisation)

Depending on the stress, the initial particle is completely replaced by fragments of a defined size. The probability for each breakage pattern or resulting fragment size is determined from breakage test results, see Figure 3. A piecewise linear regression is conducted in order to allow calculation of the replacement probability at any specific energy with linear interpolation, see Figure 5. The linear equations are implemented into the simulation software ThreeParticle from Becker3D with an API (Application Programming Interface). The relation between maximum contact force at an impact and impact velocity is determined by simulating impact tests at several velocities. Hereby, the compressive force during the whole contact process with small time steps and save intervals is evaluated, described in detail in [41, 42]. At every contact force maximum a corresponding impact velocity and a specific energy is then calculated by the API. If the maximum contact force exceeds a minimum breakage force, a random algorithm is started. At the event of breakage, one of the pre-defined breakage patterns is determined by the random generator. The probability for each breakage pattern is equivalent to the average mass fraction of the corresponding fragment size after impact at this specific energy. When the initial particle size is determined by the random generator, no replacement occurs. This leads to the correct particle size distribution in the bulk sample, when applied on a high number of particles.

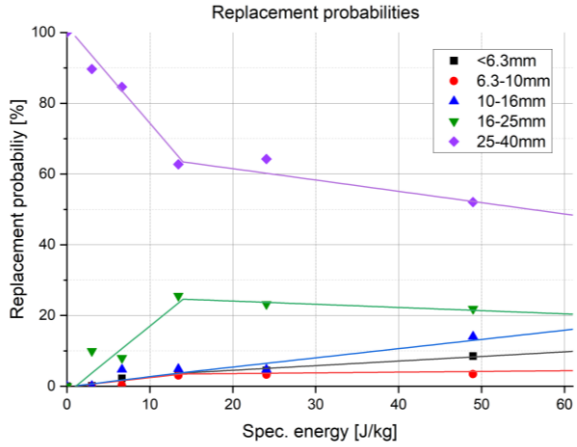

Figure 5. Replacement probabilities for following particles from piecewise linear regression based on breakage test results in Figure 3

4. VERIFICATION AND VALIDATION

The breakage model was verified with a trial of shatter tests. Hereby, a drop apparatus with a quick-opening flap was used [63], see Figure 6. The drop apparatus has a drop height of 3.8m and the bulk material is dropped onto a steel plate at the bottom. The flap is held closed by an electromagnet and is quickly opened by gravity, when triggered. 3 tests with 7.5kg and 1 test with 5.7kg blast furnace sinter of 25-40mm size were conducted. More than 4 tests would have been desirable, but could not be carried out due to a lack of material. The bulk sample is analysed before and after the test with the vibrating sorter, described in 2.1.

The test was simulated with the DE-Software ThreeParticle from Becker3D using the novel breakage model, described in 3.2. Hereby, a time step of $5x10^{-6}$s was used. Diverse material and interaction parameters for simulation were determined in [64, 65]. In Figure 7 the shatter test at different points in time is depicted. The colour scale represents the particle or fragment mass (blue=0g, red=48g). The particle breakage is clearly visible in the simulation.

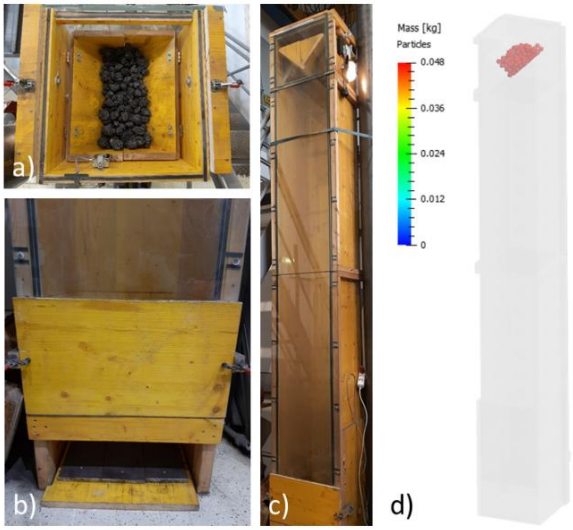

Figure 6. Drop apparatus a) bulk material in quick-opening flap b) steel plate at bottom c) front view d) DE-Simulation with ThreeParticle (Becker3D)

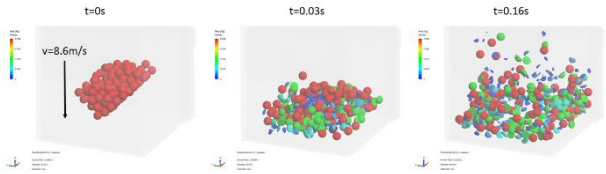

Figure 7. DE-Simulation (ThreeParticle) of shatter test using the novel probabilistic particle replacement model at different points in time

Due to the probabilistic approach, accurate simulation results require a high amount of particles. The particle mass in the shatter test is 7.5kg, which is equivalent to 160 particles with an average mass of 47g. Due to the low particle amount, the simulation was conducted 25 times and the arithmetic average of all simulations was further used. The comparison of test and simulation results from shatter tests is depicted in

Figure 8. The fragment size distribution after the drop is displayed (100% 25-40mm before the drop). Minimal mass losses are considered as fines (<6.3mm) due to dust generation and losses during fragment collection. Hereby the arithmetic average from the 4 tests and 25 simulations with standard deviations are depicted. The comparison shows a satisfying agreement of test and simulation results.

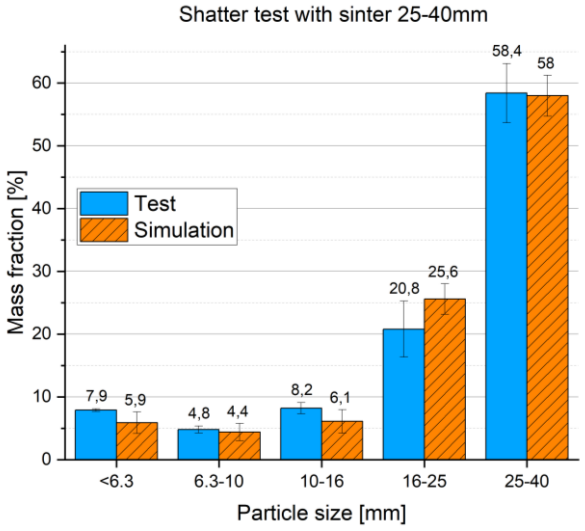

Figure 8. Comparison of test and simulation results from shatter tests

Additionally, the minimum amount of particles for sufficiently accurate simulation results with this probabilistic method was determined. Therefore, the cumulative average for each size fraction in the simulation S_i was determined and the squared deviation R_i^2 from the tests T_i was calculated with i referring to a size fraction (<6.3 to 25-40mm). The sum of the squared deviations for all size fractions is calculated after (1) and is depicted in Figure 9. The accuracy of the simulation asymptotically approaches a constant deviation from tests. In this case no significant change of simulation results is noticed over 3000 particles. Thus, a minimum of 3000 particles is required for accurate simulation results in this case.

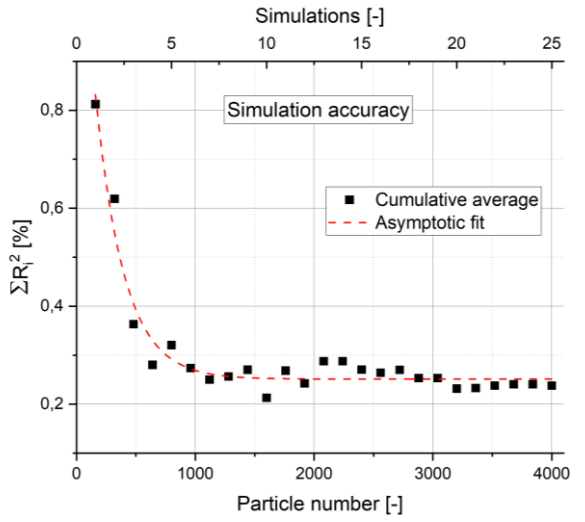

Figure 9. Evaluation of simulation accuracy in dependence of particle amount

$$\sum_{i=1}^{5} R_i^2 = \sum_{i=1}^{5} (T_i - S_i)^2 \quad (1)$$

5. APPLICATION

Bulk material degradation during conveying with two different transfer chutes at the same point was investigated. Originally, this trial was conducted to compare an innovative dynamic transfer system named FlowScrape with a standard chute with regard to particle breakage [41, 42, 66]. The dynamic transfer system FlowScrape consists of 3 rubber tracks, which are linked with cardanic joints for synchronisation and is driven by a friction wheel on the lower belt conveyor. The FlowScrape is patented [67] and described in detail in [68]. A significant reduction of bulk material degradation and in this case 50% less fines generation with the FlowScrape was noticed.

The standard chute is a simple cuboid construction with a baffle plate at the rear wall. The drop height for both systems was 1.6m and belt conveyor speeds were 1.5m/s. Sinter with 31-50mm size from a different manufacturer than in 4 was used. With each system 6 tests were conducted and the particle size distribution before and after the transfer point were measured with the vibrating sorter, described in 2.

The discrete element simulations were conducted with the software ThreeParticle from Becker3D and the same parameters as in 4 were used, see Figure 10 and Figure 12. In both simulations 465kg of sinter was used, which is equivalent to 8319 particles. The colour scale represents the particle mass. A particle mix (25, 40 and 50mm) according to the measured particle size distribution was used. Further breakage of fragments was also implemented for this case. All particles and fragments larger than 16mm are breakable. For particles smaller than 16mm no breakage was determined in breakage tests at energy levels occurring in this case. The comparison of test and simulation results is depicted in Figure 11 and Figure 13. Hereby the average of each 6 tests is calculated. The increase of mass fractions for each particle size including the standard deviations is depicted. A good agreement of test results is noticed, especially for fines generation (<6.3mm).

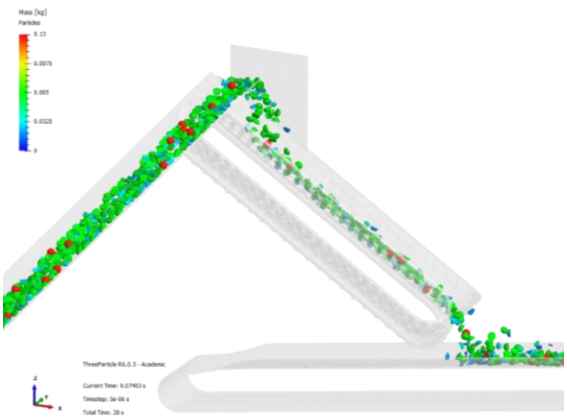

Figure 10. DE-Simulation (ThreeParticle) of the dynamic transfer system FlowScrape using the novel probabilistic particle replacement model

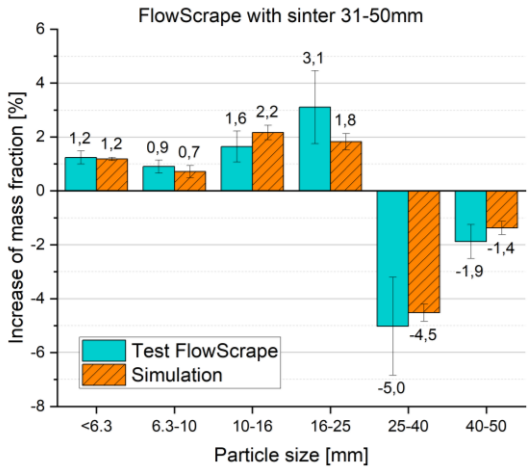

Figure 11. Bulk material degradation due to transfer with the FlowScrape. Comparison of test and simulation results.

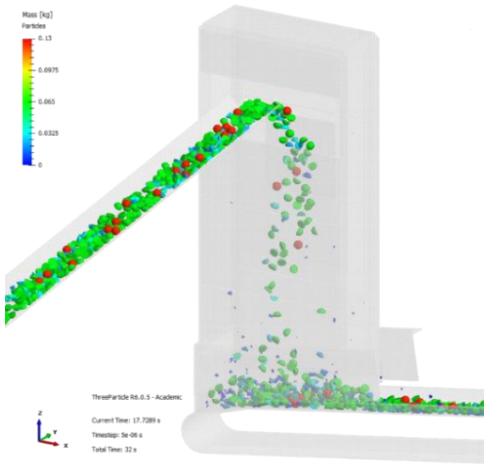

Figure 12. DE-Simulation (ThreeParticle) of standard chute using the novel probabilistic particle replacement model

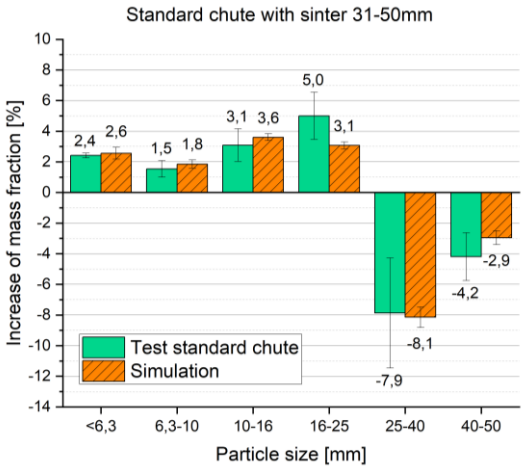

Figure 13. Bulk material degradation due to transfer with a standard chute. Comparison of test and simulation results.

6. CONCLUSION

The breakage model described in this work allows to simulate bulk material degradation during conveying processes with high mass flows. Further breakage of fragments can also be implemented to simulate long and complex processes with several damaging events. As this model is based on probabilities, a high amount of particles is required for accurate simulation results, in this case a minimum of 3000 particles. Mass and volume constancy is ensured. Any convex mesh shapes can be used as particles. Due to the convex meshed particles and sharp-edged fragments, more computing power is required than with simple spherical particles. The model has been verified and validated with a trial of shatter tests. Additional validation was carried out when applied on two different transfer chutes. As a satisfying agreement of test and simulation results was noticed, the model can be used to predict particle breakage in various applications. Especially with the here presented test method to analyse breakage characteristics, this breakage model provides an efficient way to simulate bulk material degradation.

ACKNOWLEDGMENT

This work was conducted within the project MinSiDeg, which received funding from the European Union's Research Fund for Coal and Steel (RFCS) under grant agreement number 847285.

REFERENCES

1. Fagerberg B, Sandberg N (1974) Degradation of lump ores in transport. 2nd Int. Symp. on Transport and Handling of Minerals, Rotterdam, NL
2. Kelly S, Bullock J, Smitham J et al. (1991) Fine coal generation during mining and handling. The Australian Coal Journal:31–39
3. Ooshima T, Kurihara J, Hayase K et al. (1981) Minimization of Degradation of Sintered Ore During Transportation. 3rd Int. Symp. on Agglomeration:1112–1124
4. Sahoo RK, Weedon DM (2002) Factors affecting coal degradation during handling. Bulk Solids Handling 7:282–288
5. Sahoo RK, Roach D (2005) Quantification of lump coal breakage during handling operation at the Gladstone port. Chemical Engineering and Processing:797–804
6. Sahoo RK (2007) Degradation characteristics of steel making materials during handling. Powder Technology 176:77–87. https://doi.org/10.1016/j.powtec.2007.02.013
7. Denzel M, Prenner M (2021) Minimierung des Sinterzerfalls mittels DEM (Minimization of Sinter Degradation with DEM). Berg- und Huettenmaennische Monatshefte (BHM) 166:76–81. https://doi.org/10.1007/s00501-021-01081-7
8. Goodwin PJ, Ramos CM (1987) Degradation of sized coal at transfer points. Bulk Solids Handling 7:517–537
9. Hocke H, Jones KT (1968) Factors affecting the degradation of sinter at a belt conveyor transfer point. Iron and Steel:335–340
10. Remus R, Aguado-Monsonet MA, Roudier S et al. (2013) Best available techniques (BAT) reference document for iron and steel production: Industrial emissions Directive 2010/75/EU : integrated pollution prevention and control. Scientific and technical research series, vol 25521. Publications Office of the European Union, Luxembourg
11. Nistala SH, Sinha M, Kumar Choudhary M et al. (2015) Study of generation of sinter return fines

during transportation. Ironmaking & Steelmaking 42:226–232. https://doi.org/10.1179/1743281214Y.0000000224
12. Denzel M (2022) Partikelbruch in der Fördertechnik - Prüfmethodik und Simulation mittels Diskrete Elemente Methode (Particle breakage during conveying processes - Test method and simulation with the discrete element method). In: Langefeld O (ed) 10. Kolloquium - Fördertechnik im Bergbau, 1st edn. Papierflieger Verlag GmbH, Clausthal-Zellerfeld, pp 89–101
13. Denzel M, Prenner M, Sifferlinger NA (2022) Development of an automated single particle impact tester for iron ore sinter. Minerals Engineering 175:107291. https://doi.org/10.1016/j.mineng.2021.107291
14. Schubert H (1987) Zu den Mikroprozessen des Zerkleinerns. Aufbereitungstechnik 28.5:237–246
15. Napier-Munn TJ (2005) Mineral comminution circuits: Their operation and optimisation, Repr. with minor corr. JKMRC monograph series in mining and mineral processing, vol 2. Julius Kruttschnitt Mineral Research Centre, Indooroopilly, Queensland
16. Narayanan SS, Whiten WJ (1988) Determination of comminution characteristics from single particle breakage tests and its application to ball mill scale-up. Trans. Inst. Min. Metall:115–124
17. Shi F, Kojovic T (2007) Validation of a model for impact breakage incorporating particle size effect. International Journal of Mineral Processing 82:156–163. https://doi.org/10.1016/j.minpro.2006.09.006
18. Vogel L, Peukert W (2003) Breakage behaviour of different materials—construction ofa mastercurve for the breakage probability [Vogel, Peukert]. Powder Technology 129. https://doi.org/10.1016/S0032-5910(02)00217-6
19. Vogel L, Peukert W (2004) Determination of material properties relevant to grinding by practicable labscale milling tests. International Journal of Mineral Processing 74:S329-S338. https://doi.org/10.1016/j.minpro.2004.07.018
20. Vogel L, Peukert W (2005) From single particle impact behaviour to modelling of impact mills. Chemical Engineering Science 60:5164–5176. https://doi.org/10.1016/j.ces.2005.03.064
21. Narayanan SS (1985) Development of a laboratory single particle breakage technique and its application to ball mill modelling and scale-up. PhD Thesis, The University of Queensland
22. Sahoo RK, Roach D (2004) Degradation of Coal in a Port and Shiploading Environment. PhD Thesis, Central Queensland University
23. Fandrich R, Clout J, Bourgeois F (1998) The CSIRO Hopkinson Bar Facility for large diameter particle breakage. Minerals Engineering 11:861–869. https://doi.org/10.1016/S0892-6875(98)00073-9
24. Abel F, Rosenkranz J, Kuyumcu HZ (2009) Stamped coal cakes in cokemaking technology: Part 1 – A parameter study on stampability. Ironmaking & Steelmaking 36:321–326. https://doi.org/10.1179/174328109X407112
25. Bearman RA, Briggs CA, Kojovic T (1997) The applications of rock mechanics parameters to the prediction of comminution behaviour. Minerals Engineering 10:255–264. https://doi.org/10.1016/S0892-6875(97)00002-2
26. Genc Ö (2016) An investigation on single-particle impact breakage functions of gold ore by drop-weight technique. Bulletin Of The Mineral Research and Exploration 0. https://doi.org/10.19111/bmre.78208
27. King RP, Bourgeois F (1993) Measurement of fracture energy during single-particle fracture. Minerals Engineering 6:353–367
28. Morrell S (2008) A method for predicting the specific energy requirement of comminution circuits and assessing their energy utilisation efficiency. Minerals Engineering 21:224–233. https://doi.org/10.1016/j.mineng.2007.10.001
29. Öfner W, Zaunrith G (2016) The Drop Weight Test Revisited: Characterization of the Crushability of Hot Sinter and Validation of the Approach with Natural Rocks. Berg Huettenmaenn Monatsh 161:277–282. https://doi.org/10.1007/s00501-016-0501-7
30. Quist J, Evertsson CM (2016) Cone crusher modelling and simulation using DEM. Minerals Engineering 85:92–105. https://doi.org/10.1016/j.mineng.2015.11.004
31. Tavares L, King R (1998) Single-particle fracture under impact loading. International Journal of Mineral Processing 54:1–28. https://doi.org/10.1016/S0301-7516(98)00005-2
32. Schönert K, Markstscheffel M (1986) Liberation of composite particles by single particle compression, shear and impact loading. Proceedings of the 6th European Symposium Comminution
33. Shi F, Kojovic T, Larbi-Bram S et al. (2009) Development of a rapid particle breakage characterisation device – The JKRBT. Minerals Engineering 22:602–612. https://doi.org/10.1016/j.mineng.2009.05.001
34. Zuo W, Shi F (2016) Ore impact breakage characterisation using mixed particles in wide size range. Minerals Engineering 86:96–103. https://doi.org/10.1016/j.mineng.2015.12.007
35. Mwanga A, Rosenkranz J, Lamberg P (2015) Testing of Ore Comminution Behavior in the Geometallurgical Context—A Review. Minerals 5:276–297. https://doi.org/10.3390/min5020276
36. Brown G.J. MN (1995) Applied fractal geometry in impact pulverization. The XIX International Mineral Processing Congress, San Francisco
37. Brown GJ, Miles NJ, Jones TF (1996) A fractal description of the progeny of single impact single particle breakage. Minerals Engineering 9:715–726. https://doi.org/10.1016/0892-6875(96)00063-5
38. Cavalcanti PP, Petit HA, Thomazini AD et al. (2021) Modeling of degradation by impact of individual iron ore pellets. Powder Technology 378:795–807. https://doi.org/10.1016/j.powtec.2020.10.037
39. Meier M, John E, Wieckhusen D et al. (2008) Characterization of the grinding behaviour in a single particle impact device: studies on pharmaceutical powders. Eur J Pharm Sci 34:45–55. https://doi.org/10.1016/j.ejps.2008.02.120
40. Waidbacher B (2022) Automatische Beschickung eines Prüfstandes für Hochofensinter (Automated particle feeding of a test rig for blast furnace sinter). Master's Thesis, University of Leoben
41. Denzel M, Prenner M (2021) Dynamisches Übergabesystem zur Reduktion des Partikelbruchs

(Dynamic transfer system to reduce particle breakage). 25. Fachtagung Schüttgutfördertechnik 2021:233–242. https://doi.org/10.25673/36794
42. Denzel M, Prenner M (2022) Partikelbruchvorhersage an einem dynamischen Übergabesystem und Vergleich mit einer herkömmlichen Schurre mittels DEM (Particle breakage prediction on a dynamic transfer system and comparison with a conventional chute using DEM). Berg Huettenmaenn Monatsh 167:66–75. https://doi.org/10.1007/s00501-022-01197-4
43. Delebarre A, Leroy J, Negro P (1999) Mechanical strength characterization of feed materials used in iron-making industry by Epstein theory. Powder Technology 105:95–105. https://doi.org/10.1016/S0032-5910(99)00123-0
44. Epstein B (1948) Logarithmico-Normal Distribution in Breakage of Solids. Ind Eng Chem 40:2289–2291. https://doi.org/10.1021/ie50468a014
45. Norgate TE, Tompsitt DF, Batterham RJ (eds) (1986) Computer simulation of the degradation of lump ores during transportation and handling
46. Tavares L, King R (2002) Modeling of particle fracture by repeated impacts using continuum damage mechanics. Powder Technology 123:138–146. https://doi.org/10.1016/S0032-5910(01)00438-7
47. Tavares LM, Carvalho RM de (2011) Modeling ore degradation during handling using continuum damage mechanics. International Journal of Mineral Processing 101:21–27. https://doi.org/10.1016/j.minpro.2010.07.008
48. Cleary P (2001) Modelling comminution devices using DEM. Int J Numer Anal Meth Geomech 25:83–105. https://doi.org/10.1002/1096-9853(200101)25:1<83:AID-NAG120>3.0.CO;2-K
49. Barrios GK, Pérez-Prim J, Tavares LM (2015) DEM simulation of bed particle compression using the particle replacement model. Proceedings 14th European Symposium on Comminution and Classification
50. Barrios GK, Jiménez-Herrera N, Tavares LM (2020) Simulation of particle bed breakage by slow compression and impact using a DEM particle replacement model. Advanced Powder Technology 31:2749–2758. https://doi.org/10.1016/j.apt.2020.05.011
51. Jiménez-Herrera N, Barrios GK, Tavares LM (2017) Comparison of breakage models in DEM in simulating impact on particle beds. Advanced Powder Technology 29:692–706. https://doi.org/10.1016/j.apt.2017.12.006
52. Bono JP de, McDowell GR (2016) The fractal micro mechanics of normal compression. Computers and Geotechnics 78:11–24. https://doi.org/10.1016/j.compgeo.2016.04.018
53. Cil MB, Buscarnera G (2016) DEM assessment of scaling laws capturing the grain size dependence of yielding in granular soils. Granular Matter 18. https://doi.org/10.1007/s10035-016-0638-9
54. Barrios GK, Tavares LM (2016) A preliminary model of high pressure roll grinding using the discrete element method and multi-body dynamics coupling. International Journal of Mineral Processing 156:32–42. https://doi.org/10.1016/j.minpro.2016.06.009
55. Cleary PW, Sinnott MD (2015) Simulation of particle flows and breakage in crushers using DEM: Part 1 – Compression crushers. Minerals Engineering 74:178–197. https://doi.org/10.1016/j.mineng.2014.10.021
56. Delaney GW, Morrison RD, Sinnott MD et al. (2015) DEM modelling of non-spherical particle breakage and flow in an industrial scale cone crusher. Minerals Engineering 74:112–122. https://doi.org/10.1016/j.mineng.2015.01.013
57. Potyondy DO, Cundall PA (2004) A bonded-particle model for rock. International Journal of Rock Mechanics and Mining Sciences 41:1329–1364. https://doi.org/10.1016/j.ijrmms.2004.09.011
58. Sousani M, Chagas A, Saxena A et al. (2019) Simulation of Surface Damage and Body Breakage by using DEM
59. Tavares LM, das Chagas AS (2021) A stochastic particle replacement strategy for simulating breakage in DEM. Powder Technology 377:222–232. https://doi.org/10.1016/j.powtec.2020.08.091
60. Kumar S, Kurtz SK (1993) Properties of a two-dimensional Poisson-Voronoi tesselation: A Monte-Carlo study. Materials Characterization 31:55–68. https://doi.org/10.1016/1044-5803(93)90045-W
61. Kumar S, Kurtz SK (1994) Simulation of material microstructure using a 3D voronoi tesselation: Calculation of effective thermal expansion coefficient of polycrystalline materials. Acta Metallurgica et Materialia 42:3917–3927. https://doi.org/10.1016/0956-7151(94)90170-8
62. Riedinger R, Habar M, Oelhafen P et al. (1988) About the Delaunay-Voronoi tesselation. Journal of Computational Physics 74:61–72. https://doi.org/10.1016/0021-9991(88)90068-X
63. Grübler C (2020) Evaluierung ausgewählter passiver staubreduktionsmaßnahmen beim Schüttgutumschlag an fördertechnischen Anlagen (Evaluation of passive dust reducing measures at bulk material handling on conveying equipment). PhD Thesis, University of Leoben
64. Brugger M (2021) Rücksprungverhalten von Hochofensinter (Rebound behaviour of blast furnace sinter). Bachelor Thesis, University of Leoben
65. Prenner M (2018) Simulationsparameterstudie - Sinterbunker (Simulation parameter study - Sinter bunkers). Project report, University of Leoben
66. Wagner P (2022) Vergleich zweier Übergabeeinrichtungen in Bezug auf Partikelbruch (Comparison of two transfer systems with regard to particle breakage). Master's Thesis, University of Leoben
67. Dünnwald W, Prenner M (2019) Vorrichtung zum Leiten eines von einem Abwurfende oder Austragsende einer Fördereinrichtung abfließenden Materialstroms (Device for guiding a material flow flowing out from a discharge end or delivery end of a conveying apparatus). Patentnr. DE 10 2019 108 687 A1. Deutschland
68. Prenner M (2021) Dynamische Übergabeschurre zur Effizienzsteigerung von Gurtbandförderern (Dynamic Transfer Chute to Improve Efficiency of Belt Conveyors). Berg Huttenmannische Monatshefte:1–6. https://doi.org/10.1007/s00501-021-01084-4

